Rainfall recharge thresholds decrease after an intense fire over a near-surface cave at Wombeyan, Australia

Christina Song[1], Micheline Campbell[2,1] and Andy Baker[1,3]

[1]Earth and Sustainability Science Research Centre, School of Biological, Earth and Environmental Sciences, UNSW, Sydney 2052, Australia
[2]Climate Geochemistry Department, Max Planck Institute for Chemistry, Mainz, Germany
[3]ANSTO, Lucas Heights, Australia

Correspondence to: Andy Baker (a.baker@unsw.edu.au)

Abstract. Quantifying the amount of rainfall needed to generate groundwater recharge is important for the sustainable management of groundwater resources. Here, we quantify rainfall recharge thresholds using drip loggers situated in a near-surface cave: Wildman's cave at Wombeyan, southeast Australia. In just over two years of monitoring, 42 potential recharge events were identified in the cave, approximately 4 m below land surface which comprises a 30° slope with 37% bare rock. Recharge events occurred within 48 hours of rainfall. Using daily precipitation data, the median 48 h rainfall needed to generate recharge was 19.8 mm, without clear seasonal variability. An intense experimental fire experiment was conducted 18 months into the monitoring period: the median 48 h rainfall needed to generate recharge was 22.1 mm before the fire (n=22) and 16.4 mm after the fire (n=20), with the decrease in rainfall recharge most noticeable starting three months after the fire. Rainfall recharge thresholds and number of potential recharge events at Wildman's Cave are consistent with those published from other caves in water-limited Australia. At Wildman's Cave, we infer that soil water storage, combined with the generation of overland flow over bare limestone surfaces is the pathway for water movement to the subsurface via fractures and that these determine the rainfall recharge threshold. Immediately after the fire, surface ash deposits initially retard overland flow, and after ash removal from the land surface, soil loss and damage decrease the available soil water storage capacity, leading to more efficient infiltration and a decreased rainfall recharge threshold.

1 Introduction

Groundwater recharge is a vital process where freshwater replenishes itself to support and nurture a healthy ecosystem and provide a source of water for human use. The groundwater recharge process is strongly controlled by climatic and geologic factors in association with temporal variability (Ajami, 2021). In warmer climates, evapotranspiration of water can occur at a faster rate than it can be replenished by rainfall, limiting the occurrence of recharge to infrequent, high magnitude rainfall events (for example, Boas and Mallants, 2022). In lithologies that have low permeability, recharge is limited to preferential flow pathways such as fractures, leading to a very low fraction of annual rainfall generating recharge (Kotchoni et al., 2019).

Quantifying both the timing and amount of groundwater recharge is a challenge, yet fundamentally important if changes in groundwater recharge over time are to be quantified (e.g. Noori et al., 2023). At the event scale, only a few techniques are

available to identify recharge, and the source and age of the water being analysed is often uncertain. Recharge events can be identified in some groundwater wells or bores where fluctuations in groundwater level can be observed over time using the water table fluctuation method (Healy and Cook, 2002). Recently, a new approach has been proposed that uses loggers in underground spaces such as caves that are situated in the unsaturated zone (Baker et al., 2020, 2021). This approach identifies when water percolates into the subsurface void and has been proposed as another method for identifying both the timing of recharge events at the event scale and the amount of rainfall needed for caves, tunnels and mines (Baker et al., 2024).

Fire can have an impact on subsurface hydrology, however its role in recharge processes is less well understood. For example, ash beds have a variable impact on hydrology and have been shown both to increase runoff and reduce infiltration (e.g. Gabet and Sternberg, 2008) and store water, increasing infiltration (e.g. Woods and Balfour, 2008), and in general ash has a higher capacity to hold water than soil (Bodí et al., 2014). However, the formation of ash crusts may enhance overland flow and impede infiltration (Balfour et al., 2014; Onda, 2008). Ash crusts are thought to form due to physical-chemical properties of ash as well as rainfall compaction. Ashes which contain oxides (well-combusted ashes) may form ash crusts due to the hydration and recrystallisation of carbonate crusts (Balfour et al., 2014; Bodí et al., 2014). These crusts are generally ephemeral, but post-fire changes to hydrology may persist for several years (Cerdá, 1998). Furthermore, ash can clog soil pores, further reducing infiltration capacity (Bodí et al., 2014; Woods and Balfour, 2008).

Here, we use the unsaturated zone monitoring approach that uses loggers in underground spaces to investigate the potential impacts of fire on the amount of rainfall needed to generate recharge. Between December 2014 and May 2017, before and after a fire, cave drip water hydrological monitoring was undertaken at a shallow cave site in southeast Australia as part of a wider investigation of the impacts of fire on karst processes. The experimental design was to have at least one year of monitoring data before and after a fire, to assess potential impacts on the cave environment. Hydrograph analysis and percolation water geochemical analyses from that study were published by Bian et al. (2019), however, the amount of rainfall needed to generate recharge using cave percolation waters was not determined. Bian et al. (2019) demonstrated percolation water events into the cave were characterized by hydrographs of shorter duration and with higher maxima after the fire. Combined with inorganic geochemical and water isotope data, this observation was interpreted as increased preferential (fracture) flow and decreased diffuse flow (from the soil) after the fire. Because Bian et al. (2019), did not analyse the hydrology data to obtain rainfall recharge thresholds for each potential recharge event, this analysis is undertaken here, to (1) quantify the rainfall recharge threshold for the site (2) to investigate seasonal variations in rainfall recharge threshold and the possible impact of surface fire on rainfall recharge thresholds and (3) compare results to those reported from sites in southern and eastern Australia (Baker et al., 2020, 2021).

2 Site Description and Methods

Wildman's Cave is located at 608 m above sea level in the Wombeyan Caves Karst Conservation Reserve (34° 19″ S, 149° 58″ E), in the south-eastern part of New South Wales, Australia (Fig. 1). It is formed in the Silurian age Wombeyan Limestone formation, a marble which is highly fractured with no matrix porosity remaining (Osborne, 1993). Subsurface water movement is therefore dominated by fracture and conduit flows. The cave is small and shallow with a narrow pothole type entrance and a total of 42 m of cave passage containing numerous stalactites (Wylie and Wylie, 2004). The cave is approximately 4 m below the land surface. The surface above the cave comprises a 30° sloping ridgeline. 37% of the surface has no soil cover,

71 the remaining land surface has a median 5 cm soil cover, reaching a maximum 33 cm where soil has accumulated in fractures.
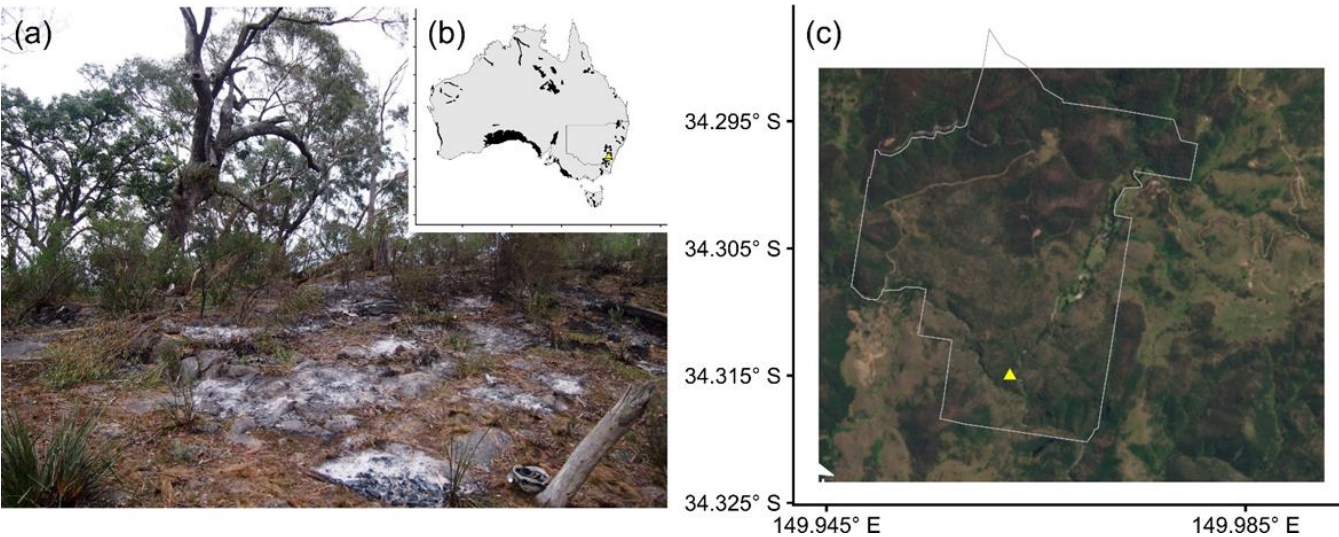72 Vegetation, where present, comprises dry sclerophyll shrubs and grasses.
73

75 **Figure 1**. a). Photograph of the surface above the cave one day after the fire (source: Andy Baker). b) Australia with karst overlay (black),
76 yellow triangle indicates the study site (WOKAM; from Chen et al (2017). c) Sentinel S2 visible image, with outer bounds of the Wombeyan
77 Karst Reserve. SentinelS2 True Colour image [2024]. Retrieved from Copernicus Dataspace [7 December 2024], processed by Copernicus.
78 Wombeyan karst conservation reserve boundary: State Government of NSW and NSW Department of Climate Change, Energy, the
79 Environment and Water 2000, NSW National Parks and Wildlife Service (NPWS) Estate, accessed from The Sharing and Enabling
80 Environmental Data Portal [https://datasets.seed.nsw.gov.au/dataset/9bad468a-c2a6-4c90-bfaa-8ae8af72e925], date accessed 2024-11-07.
81

82

83 Annual precipitation at the site over the last ten years has a long-term average of 802 mm, annual areal potential
84 evapotranspiration (PET) is 1228 mm, and modelled actual evapotranspiration (AET) is 680 mm (precipitation data is from
85 the Bureau of Meteorology (BOM) and evapotranspiration data from the Australian Water Landscape Model (AWRA-L) v7,
86 Frost and Shokri, 2021). Temperature at Taralga (17 km distant and 845 m above sea level) ranges from an average minimum
87 of 6.1 °C to an average maximum of 18.3 °C. Over the study period, precipitation at the site was close to the long-term average
88 (2015 annual precipitation: 773 mm; 2016 annual precipitation: 843 mm) and areal PET slightly higher than the long-term
89 average (2015 annual areal PET: 1307 mm; 2016 annual areal PET: 1331 mm). There is minor seasonality in precipitation,
90 with monthly precipitation in the cooler months (June and July) tending to be both lower and less variable than during the
91 warmer months (Fig. 2). We note, however, that even the cool months can report unusually high monthly totals (Fig. 2), likely
92 owing to the impact of East Coast Lows, intense low pressure systems that form off the east coast of Australia, and which are
93 most common in autumn and winter (Pepler et al., 2014).
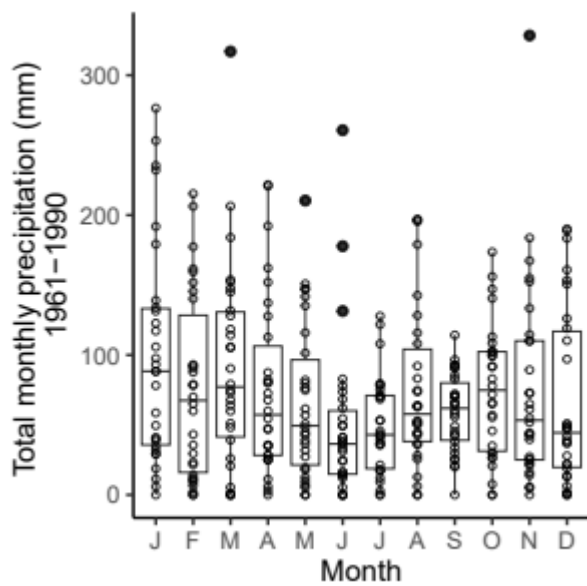94

Figure 2. Total BOM monthly precipitation, 1961-1990. Aggregated from daily rainfall data from Wombeyan Caves (BOM Station number 63093).

We used data from eleven Stalagmate © drip loggers that were deployed throughout the cave between December 2014 and January 2017 and for which hydrograph analysis has been previously presented in Bian et al. (2019). Only four loggers remained in operation from January 2017 to May 2017: data from this period was not analysed quantitatively. Monitoring ceased in May 2017, one year after an experimental fire occurred on the surface above the cave. Loggers were programmed to record the total number of drips in a 15-minute period. Recharge events were identified here through visual inspection of the time series and cross-checked with the events identified in Bian et al. (2019) and a date allocated. To determine the amount of rainfall needed to generate recharge, daily rainfall records were obtained for the six days up to and including the date of recharge. Since daily rainfall amounts are collected for the 24 hours up to 9 am, this analysis also considered precipitation on the day after recharge was observed to ensure that all contributing rainfall was included. Precipitation data was taken from the BOM station at Wombeyan Caves as well as gridded daily precipitation from the AWRA-L, accessed via the Australian Water Outlook website (Bureau of Meteorology, 2024). Where there were incomplete returns from the BOM station, the AWRA-L gridded daily precipitation value was used.

Summarizing the main results of the pre-fire and post-fire hydrological and geochemical monitoring of the site presented in Bian et al. (2019), an intense experimental fire over the cave (10 m x 10 m) occurred on 25th May 2016, which resulted in the surface litter being generally consumed by the fire, with ash accumulations of several centimetres depth occurring in places. Thermocouples placed at 12 cm depth in the soil recorded maximum temperatures between 30 and 930 °C, with spalling of the limestone and calcining observed in localised hotspots. Bian et al. (2019) analysed drip water hydrograph structure, water isotope composition and geochemistry before and after the fire. After the fire, recharge event hydrographs were peakier and of shorter duration than pre-fire. Stable water isotope composition of drip waters was relatively constant pre-fire, with a rapid shift to a more negative oxygen isotope composition immediately post-fire, returning to the pre-fire baseline after six months.

4

119   This was interpreted to be due to the complete evaporation of soil and shallow vadose zone water in the fire, with the post-fire
120   drip water isotopic compositions reflect that of the first recharge events after the fire rather than a long-term mixed precipitation
121   signal, and subsequent rainfall events over the next six months replenishing the water in the soil and shallow vadose zone.
122   Water geochemical analyses demonstrated a decrease in rock-water residence time post-fire, with an associated increase in
123   ash-derived sulphur immediately post-fire and limited evidence of other ash-derived geochemical tracers. For further details
124   see Bian et al. (2019).

125

126   To investigate whether rainfall recharge thresholds were altered by an intense experimental burn, we qualitatively compared
127   recharge thresholds calculated for the pre- and post-fire intervals. Because 48 h thresholds may be overestimated due to both
128   the coarse sampling interval and the impact of extreme events, we first compared the minimum recharge threshold calculated
129   for each month pre- and post-fire. We then quantitatively analyzed the 48 h rainfall recharge thresholds for all events before
130   and after the fire using the BOM station data. To overcome the different lengths of monitoring data before and after the fire,
131   we undertook a stratified qualitative analysis with data aggregated by season (DJF, MAM, JJA, SON) and 6-monthly periods
132   (Summer/Autumn and Winter/Spring and Autumn/Winter and Spring/Summer).

133   **3 Results**

134   Daily rainfall (BOM) and evapotranspiration (AWRA-L), and the 15-minute total number of drips averaged for all loggers are
135   shown in Figure 3. A total of 42 recharge events occurred between December 2014 to January 2017, an average of 1.6 recharge
136   events per month. One observed recharge event (4th May 2015) had only 1.6 mm of associated antecedent rainfall associated
137   with it, and we assume that this was a locally heavier event that was not captured in the gauge ~ 2 km away. This event is not
138   included in subsequent rainfall recharge threshold calculations. Recharge events occurred in all months except March, and
139   only seven recharge events were observed in the late summer / early autumn months of February to May (Fig. 4). Excluding
140   the May 2015 event, 22 recharge events were observed before the fire and another 19 after the fire. Analysis of the daily
141   rainfall distribution before and after the fire showed very little difference (Fig. 5).

142
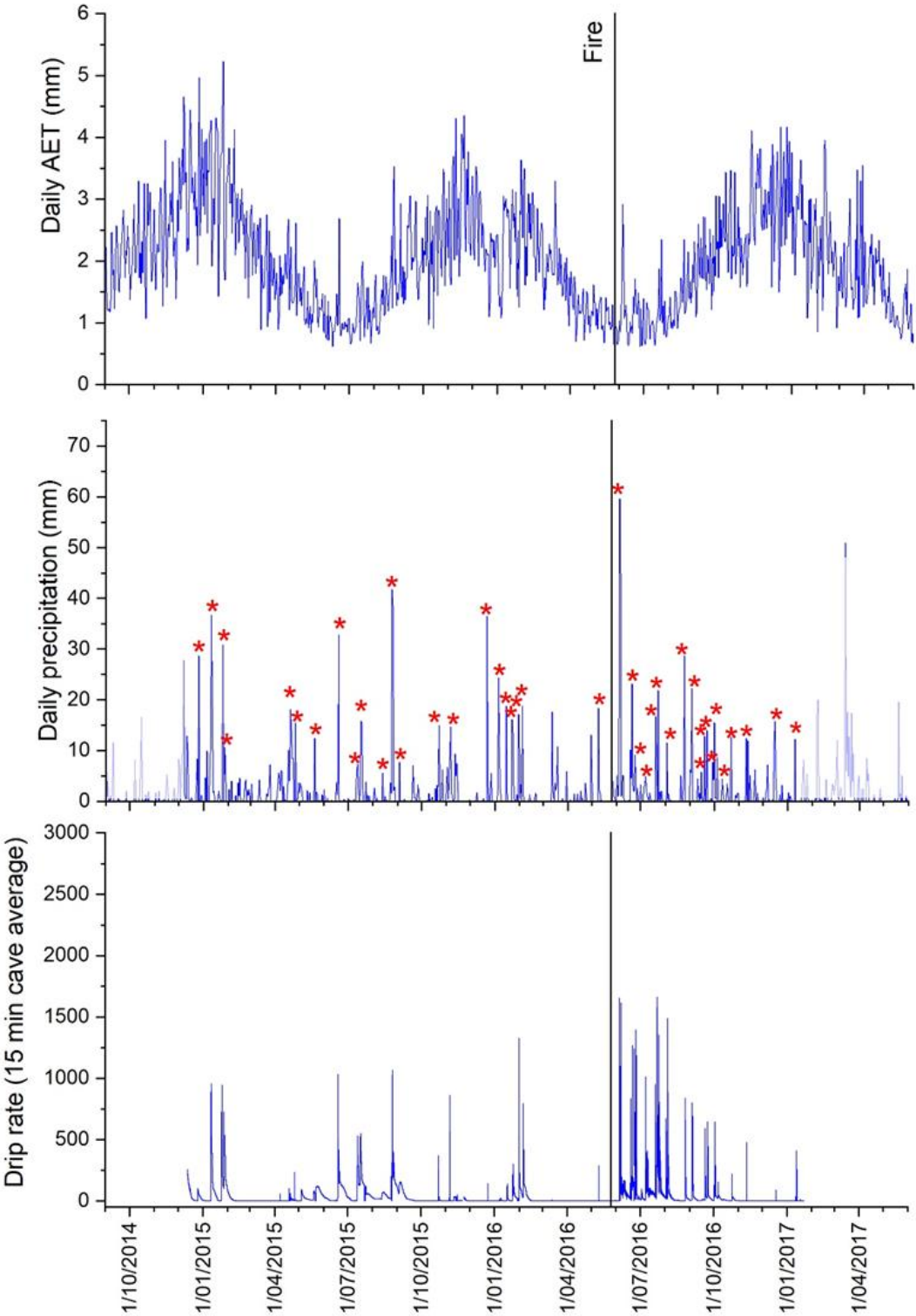
Figure 3. Daily AET (from the AWRA-L), daily precipitation (light blue when outside the monitoring period) with timing of recharge events
145 shown by red asterisks, and average 15 min total drips.

146
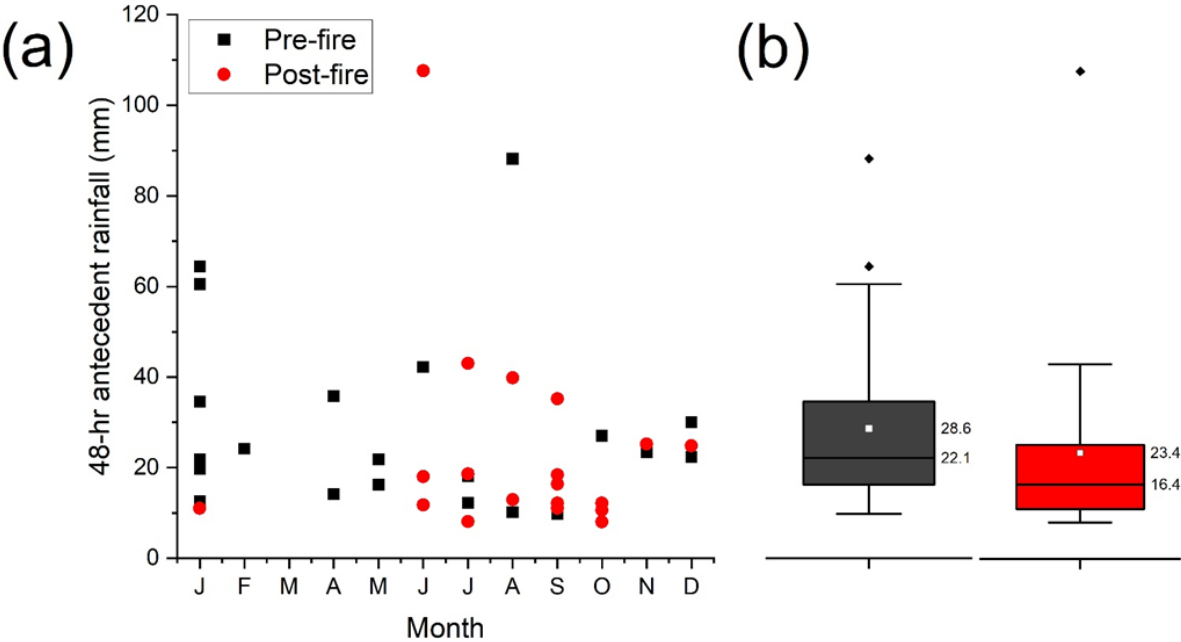
147 **Figure 4** a) 48 h antecedent rainfall classified by month and whether before or after fire. b) box and whisker plot of all 48 h rainfall amounts
148 for before the fire (black) and after the fire (red).

149

150 Five of the events occurred when there were incomplete daily precipitation returns from the BOM rain gauge and for these
151 events the gridded AWRA-L data was used. Comparison of the BOM and AWRA-L 48 h rainfall totals for those events where
152 both BOM and AWRA-L data is available (data is presented in Table 1) suggest that AWRA-L 48 h precipitation is on average
153 17% lower than the BOM gauge. No correction was applied.

154

155 Antecedent conditions were analysed for the 24, 48, 72, 96, 120 and 144 hours prior to each observed recharge event (Fig.
156 A1). Considering all recharge events, compared to the 144 (six day) sum antecedent precipitation, 48% of all precipitation
157 occurred in the first 24 hours and 69% of all precipitation occurred within the 48 hours prior to recharge. The relative

158   contribution to the total percentage rainfall over 72, 96 and 120 hours continued to decline, and therefore we use the 48 h
159   antecedent total precipitation amount to determine rainfall recharge thresholds.
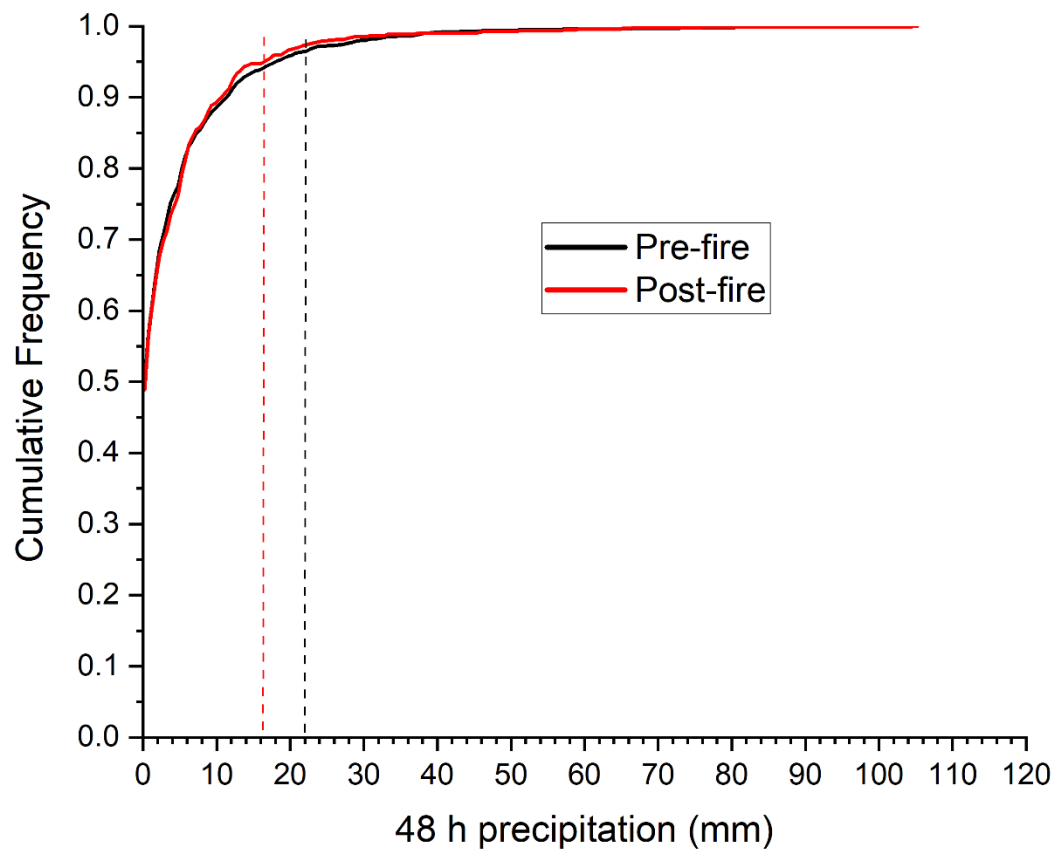

160   **Figure 5.** Cumulative frequency of 48 h precipitation pre (black) and post (red) fire. Dashed lines show the median rainfall recharge
161   thresholds.

Pre-fire				Post-fire			
Event	Date	48 h precip-itation (mm) BOM	48 h precip-itation (mm) AWRA-L	Event	Date	48 h precip-itation (mm) BOM	48 h precip-itation (mm) AWRA-L
1	25/12/2014	**22.4**	28.7	24	4/06/2016	107.6	76.1
2	11/01/2015	60.5	55.5	25	18/06/2016	**11.8**	14.8
3	24/01/2015	64.4	30.9	26	24/06/2016	18	13.6
4	27/01/2015	19.8*	19.8	27	6/07/2016	**8.1***	8.1
5	20/04/2015	35.8	32.4	28	20/07/2016	18.6	23
6	25/04/2015	**14.2**	15.5	29	22/07/2016	43	22.2
8	19/05/2015	**16.2**	14.6	30	2/08/2016	12.9*	12.9
9	18/06/2015	42.2	38.3	31	24/08/2016	39.8	33.1
10	13/07/2015	12.2	9.8	32	2/09/2016	35.2	28
11	16/07/2015	18.1*	18.1	33	14/09/2016	11	6.3
12	12/08/2015	**10.2**	5.9	34	18/09/2016	16.4	13.9
13	25/08/2015	88.2	80.5	35	21/09/2016	18.4	16.6
14	3/09/2015	**9.8**	8	36	29/09/2016	12.2	12.1
15	22/10/2015	27	20.8	37	4/10/2016	10.6	9.1
16	5/11/2015	**23.4**	23.6	38	11/10/2016	**8**	6.4
17	21/12/2015	30	36.6	39	22/10/2016	12.2	12.7
18	6/01/2016	12.6	13.1	40	9/11/2016	25.2	13.7
19	15/01/2016	20.3*	20.3	41	16/12/2016	24.8	20.5
20	21/01/2016	21.8	16.2	42	10/01/2017	**11**	12.3
21	29/01/2016	34.6	17.2				
22	4/02/2016	24.2	20.9				
23	8/05/2016	21.8	18.4				

162

Table 1. Summary of recharge events. Data with asterisks: incomplete returns for the BOM station on these dates. AWRA-L data was used. Recharge event 7 occurred on 4th May 2015 and was a local rainfall event not captured in the gauge. The monthly minimum recharge thresholds presented in Figure 6 are in bold.

The 48 h rainfall recharge thresholds for all events are presented in Table 1. Fig. 4 presents the rainfall recharge thresholds, plotted by month and whether before or after the fire (Fig. 4a) and for all recharge events (Fig. 4b) using data from the BOM

gauge. The median 48 h rainfall recharge threshold is 19.8 mm (mean: 26.2 mm). The lowest minimum 48 h rainfall recharge threshold was 8.0 mm, observed after the fire in July and September, and the highest minimum was 25.2 mm, observed after the fire in November. Comparison between rain gauge and AWRA-L gridded daily precipitation yielded similar rainfall recharge thresholds (AWRA-L median: 17.2 mm; mean 22.0 mm).
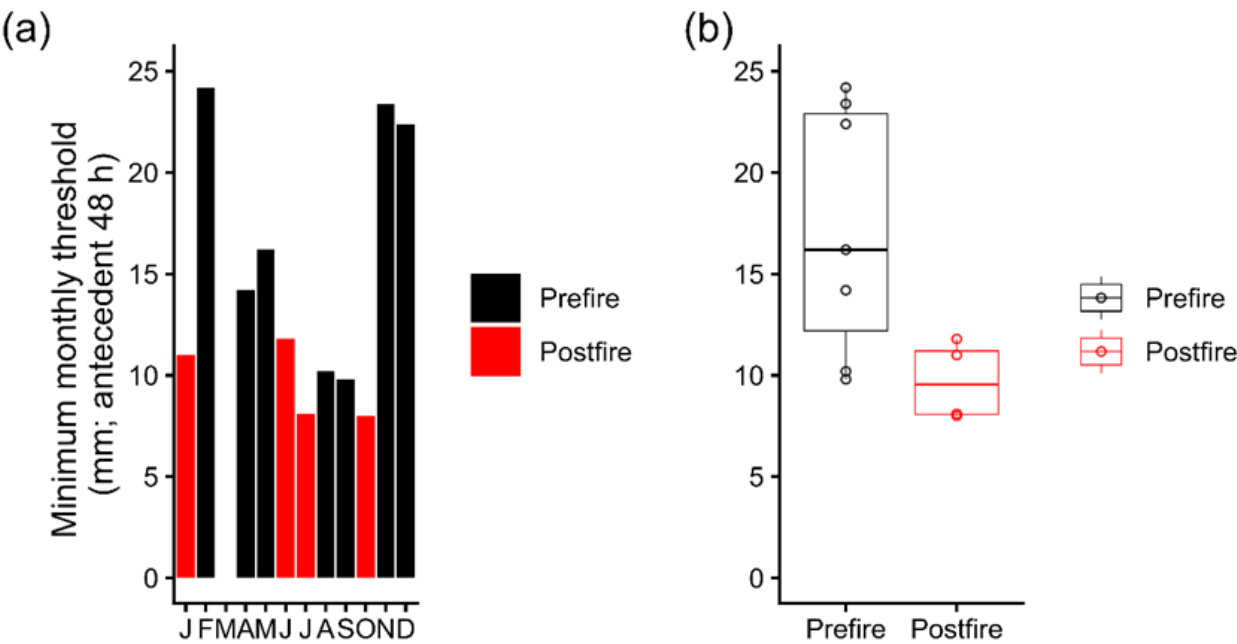

Figure 6: Minimum 48 hr precipitation required for recharge to occur for each month. Black indicates that the minimum recharge threshold occurred pre-fire, while red indicates that the minimum recharge threshold occurred post-fire. These values are bolded in Table 1.

48 h rainfall recharge thresholds were compared before and after the fire. Fig. 6 shows a qualitative reduction in the recharge threshold postfire using the minimum recharge in each month. The median 48 h rainfall needed to generate recharge was 22.1 mm before the fire (n=22) and 16.4 mm after the fire (n=19) (Fig. 7a). The pre- and post-fire monitoring periods were of different lengths, with no reliable post-fire monitoring in the late summer / early autumn of 2017, when rainfall recharge thresholds might be expected to be higher due to enhanced evapotranspiration, and a Kruskal-Wallis ANOVA indicates these rainfall recharge thresholds are not significantly different at the 95% level.

Considering December to February (DJF, summer), March to May (MAM, autumn), June to August (JJA, winter) and September to November (SON; spring)) there is qualitative evidence of a reduction in the post-fire recharge threshold in spring (SON) and summer (DJF) (Fig. 7b) (noting that there were 10 pre-fire events and 2 post-fire events in DJF, and 3 pre-fire events and 9 post-fire events in SON). Aggregating these seasonal values into coarser categories (e.g. Summer/Autumn and Winter/Spring, Fig. 7c; and Autumn/Winter and Spring/Summer, Fig. 7d) highlights a reduction in the post-fire recharge threshold relative to the pre-fire threshold in both the Spring/Summer (3-9 months post fire) and Summer/Autumn (6-12

months post fire) categories, although the difference is more pronounced in the Spring/Summer data. While the Summer/Autumn and Winter/Spring categories are unevenly sampled, the Autumn/Winter and Spring/Summer categories are evenly sampled. Trends in the seasonal data are robust to the source of the precipitation information, identified in the thresholds calculated from both the BOM data (Fig.7) and the AWRA-L data (Fig. A2).
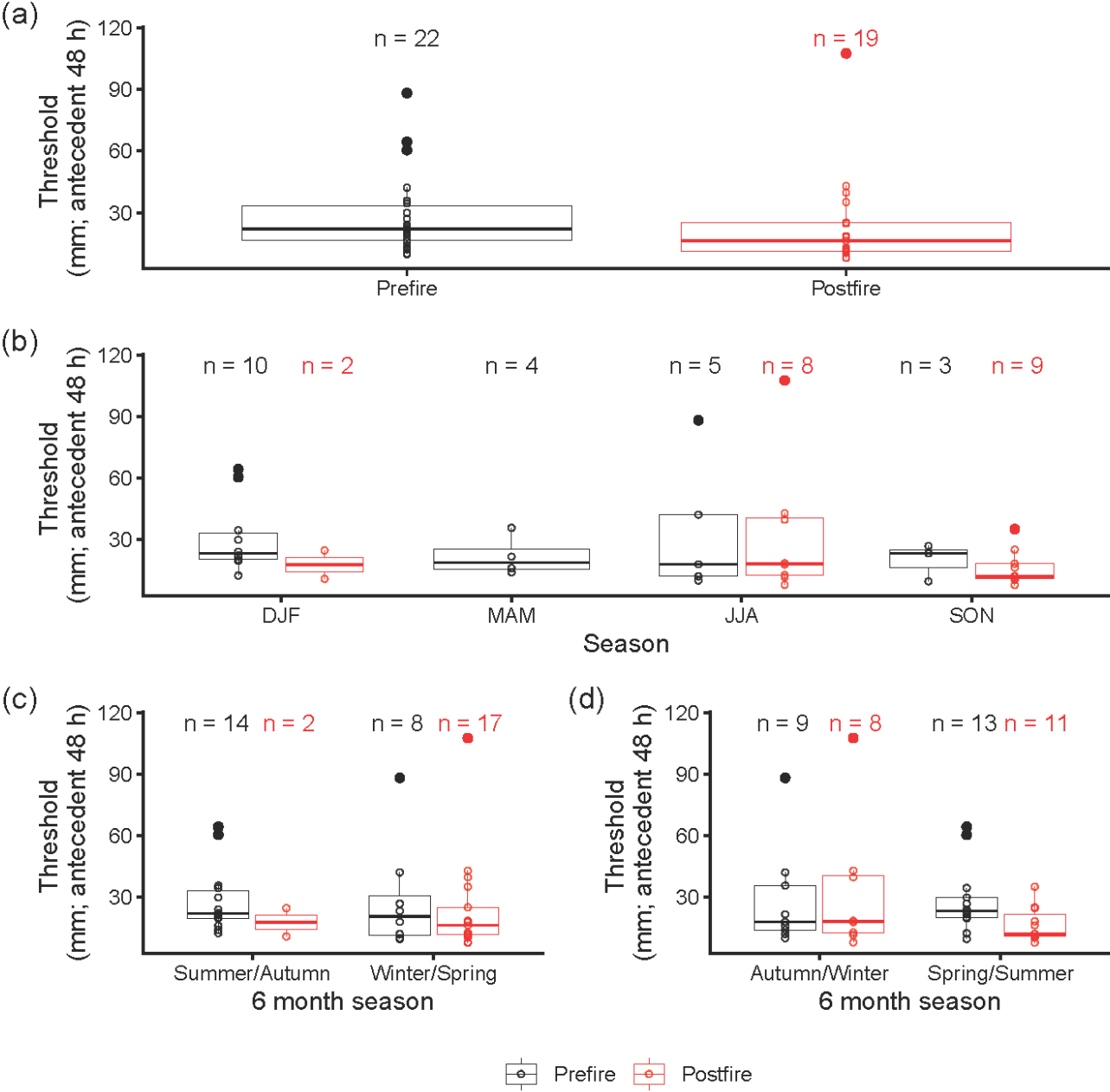
196 **Figure 7**. Comparison of recharge thresholds pre-and post-fire using BOM data. A) all recharge events B) all recharge events grouped by
197 three-month season C) all recharge events grouped by six-month seasons summer/autumn and winter/spring D) all recharge events grouped
198 by six-month seasons autumn/winter and spring/summer. Note that sample sizes are different depending on seasonal grouping, most
199 comparable for panel d, where Autumn/Winter have 9 samples for pre-fire, 8 samples for post-fire, and spring/summer have 13 samples for
200 pre-fire, 11 samples for post-fire.

4 Discussion

202 Figure 5 demonstrated very little difference in the daily rainfall distribution before and after the fire, indicating that these
203 differences in rainfall recharge thresholds is unlikely to be due to differences in daily precipitation. The median rainfall
204 recharge threshold at Wildman's Cave (19.8 mm in 48 h) is comparable to two other temperate climate sites using the same
205 methodology in south east Australia (Table 2). 41-67 mm/week of precipitation was needed before recharge occurred at the
206 South Glory Cave, Yarrangobilly, Australia (Baker et al., 2021). 76-79 mm/week of precipitation was needed in caves in the
207 Macleay region of New South Wales (Baker et al., (2020). The number of potential recharge events per year (20 per year)
208 observed at Wildman's Cave is at the upper end of the range reported previously, with the most similar characteristics at
209 monitoring site LR1 at Yarrangobilly, which had the most recharge events per year for that site (17) and the lowest rainfall
210 recharge threshold (41 mm/week of precipitation) (Table 2).

Site	Climate (Köppen-Geiger)	Annual Precipitation (mm)	Lithology	Soil and vegetation	Number of events / year	Median 7-day rainfall recharge threshold (mm)	Median 48 h rainfall recharge threshold (mm)
Upper and Lower Macleay Caves, NSW 2014-2019	Cfa	1218	Permian limestone	Subtropical rainforest to dry subtropical rainforest	3.8 to 5.4	76 to 79	*52 to 54* *
South Glory Cave, NSW 2013-2019	Cfb	1102	Silurian limestone	Red clays, thin lose soils and bare rock with sub-alpine open snow gum woodland	3.5 to 17	41 to 67	*28 to 46* *
Wildman's Cave, NSW 2014-2017	Cfb	802	Silurian marble	Bare to patchy soil, native shrubs and grasses	20		19.8

212 *inferred assuming 69% of precipitation is within 48 h of the recharge event

213 **Table 2.** Site info data from Baker et al. (2020, 2021) and this study. Cfa: temperate, no dry season, hot summer. Cfb: temperate, no dry
214 season, warm summer.
215

The effect of the intense fire on the rainfall recharge threshold is evident, with a decrease in the amount of rainfall needed post-fire, with this most evident in spring / summer, from three months after the fire. The decreased rainfall recharge threshold coincides with changed hydrograph characteristics observed by Bian et al. (2019), where post-fire recharge event hydrographs had higher peaks and were of shorter duration. Bian et al. (2019) also observed a rapid post-fire shift in cave drip water stable isotope (δ^2H, δ^{18}O) composition, interpreted as indicating that significant loss of existing soil and near-surface karst water had occurred during the fire due to evaporation. The isotope data took six months to return to the pre-fire baseline, suggesting that the epikarst water stores took six months to replenish and mix. Only limited evidence of ash-derived solutes was observed in the drip water post-fire, interpreted as an effect of volatilisation due to fire intensity.

We hypothesise that a post-fire loss of soil water storage would allow runoff generation to be more effective across areas of bare limestone to the zones of focused recharge (Fig. 8). These observations are consistent with the post-fire response in surface streams, which can include an increase in peak flow rates post-fire (Scott and Van Wyk, 1990), noting that the post-fire response of surface streams is variable and site specific (Moody et al., 2013). Figure 8A presents our conceptualisation of the pre-fire hydrology, with patchy soil and soil filled fractures retarding overland flow and storing water. Recharge occurs when overland flow occurs to focused recharge zones. The decrease in rainfall recharge threshold is not observed immediately post-fire, when the land surface above the cave was covered with thick ash deposits (see Fig. 1). Our observations at the site showed a thick and widespread ash cover immediately post-fire (Fig.1) which was absent four months post-fire (Fig. A3), with bare rock and absence of shrubby vegetation observed one year post-fire (Fig. A4). This is compatible with the presence of ash produced by the high-severity experimental burn, combined with the moderate rainfall experienced in the days immediate post-fire (10.4 mm in the week following the experimental fire), resulting in the formation of an ash crust. The presence of an ash crust (Figure 8B), combined with clogging of any remaining soil pores, is likely to have altered overland flow pathways to the recharge zones (Woods and Balfour, 2008; Balfour et al., 2014). Bian et al. (2019) demonstrate that recharge events at this time had peakier and shorter duration hydrographs and an altered water isotope composition than pre-fire (Bian et al. 2019). We conceptualise this period as one where recharge and associated recharge thresholds could be impacted by the ash cover, and when recharge occurred, it was through fractures that were relatively free of soil, vegetation and water and which had been potentially widened during the fire.

When this ash was subsequently transported from the surface above the cave, as observed four months after the fire (Fig. A3), the loss of the retarding effects of the ash crust, combined with the effect of soil removal and karst fracture enhancement, leading to enhanced infiltration and consistently resulted in reduced rainfall recharge thresholds (Figure 8C). Recharge events that occurred at this time still had peakier and shorter duration hydrographs than pre-fire (Bian et al., 2019) due to the loss of surface soil and increased area of bare rock and associated loss of soil storage and retardation of overland flow. Drip water isotope composition during this post-fire period returns to the pre-fire baseline, indicative of the replenishment of water in subsurface karst fractures and voids. Despite this replenishment, the combination of peakier and short duration hydrographs and decreased rainfall recharge thresholds suggests a longer-term change in hydrology, due to soil loss, increased bare rock, and widened fractures, the combination of which enhanced overland flow and fracture flow.

A. Before the fire   B. <3 months post fire   C. >3 months post fire

OF

soil

soil filled
fracture

R
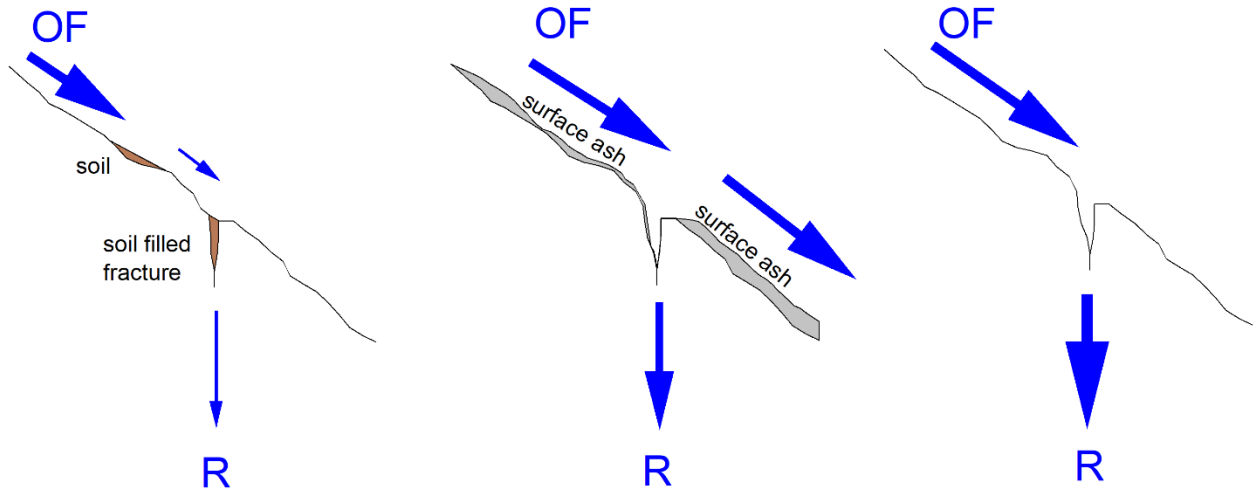
Patchy soil and soil fillled
fractures hold water.

When the rainfall recharge
thehold is exceeded, overland
flow (OF) to focused recharge
zones occurs and recharge (R)
occurs.

OF

surface ash

surface ash

R

Widened fractures.

Formation of ash crust.

Loss of soil and vegetation.

OF is promoted, rainfall
recharge thresholds start to
increase.

OF

R

Ash bed eroded.

Continued loss of soil and
vegetation.

OF is more effective with less
soil cover.

Recharge threshold is
consistently lower.

Figure 8. Conceptual figure of the recharge processes (A) before the fire (B) less than three months after the fire and (C) more than three months after the fire.

Pre- and post-fire hydrological datasets, such as ours, that can be used to calibrate or validate water balance models of groundwater recharge are rare (Guzmán-Rojo et al., 2024). Our data provides quantified information on the evolution of the post-fire response, including the length of time post-fire where surface ash enhanced overland flow and limited recharge, and the subsequent decreased rainfall recharge threshold due to soil loss and enhanced fracturing that occurred after the ash had been transported from the land surface. This hydrological response is consistent with ParFlow simulated surface and subsurface water balance changes for a water limited site and high fire severity (Atchley et al., 2018).

5 Conclusions

Our results from Wildman's Cave, with a median 48 h rainfall recharge threshold of 19.8 mm and 20 events per year, falls at the lower end of the range of previously observed rainfall recharge thresholds and higher end of the range for the number of potential recharge events per year across sites in temperate southern and eastern Australia, which have a median 48 h rainfall recharge greater than 28 mm and less than 17 events per year. Future studies should investigate these recharge characteristics across a diverse range of sites.

We provide direct measurements of the impact on fire on the potential for groundwater recharge, observing a delayed decrease in the rainfall recharge threshold occurring three months after a severe fire. The delayed change to the threshold is likely due to the presence of a thick ash bed, which likely prevented infiltration of precipitation. While we have demonstrated that a severe wildfire results in a lower recharge threshold, it is unknown whether a less-intense fire would have a similar effect. Similarly, this investigation was limited to three years of monitoring, and it is also not known whether this change in recharge threshold is permanent, or if the system will return to 'pre-fire' conditions following vegetation regrowth. Future work should aim to replicate this study with fires of different severities, and should include hydrological monitoring for some years after vegetation regrowth.

Competing interests
The authors declare that they have no competing interests

Data availability
The hydrology data is available at 10.6084/m9.figshare.28169672. All other hydroclimate datasets are publicly available from the Australian Bureau of Meteorology Climate Data Online (http://www.bom.gov.au/climate/data/) and Australian Water Outlook webpages (https://awo.bom.gov.au/). The karst area overlay used in Figure 1 is available at doi: 10.25928/b2.21_sfkq-r406, the map concept is described in Chen et al., 2017. The Sentinel S2 visible image used in Figure 1 was retrieved from the Copernicus Dataspace (https://dataspace.copernicus.eu/explore-data/data-collections/sentinel-data/sentinel-2). The Wombeyan boundary is available from New South Wales government The Sharing and Enabling Environmental Data Portal [https://datasets.seed.nsw.gov.au/dataset/9bad468a-c2a6-4c90-bfaa-8ae8af72e925]. The digital elevation model is available from NSW Government, DFSI Spatial Services and accessed via Elvis - Elevation and Depth - Foundation Spatial Data (https://elevation.fsdf.org.au/).

Author contributions

CS performed initial data analysis and interpretation, MC provided additional data analysis and interpretation. AB undertook additional data analysis and wrote the first manuscript draft with contributions from all authors.

References

Ajami, H.: Geohydrology: Groundwater. Encyclopedia of Geology (Second Edition). D. Alderton and S. A. Elias. Oxford, Academic Press, 408-415, 2021.

Atchley, A.L., Kinoshita, A.M., Lopez, S.R., Trader, L., and Middleton, R.: Simulating Surface and Subsurface Water Balance Changes Due to Burn Severity. Vadose Zone J. 17, 180099, https://doi.org/10.2136/vzj2018.05.0099, 2018

Baker, A., Berthelin, R., Cuthbert, M.O., Treble, P.C., Hartmann, A. and the KSS Cave Studies Team: Rainfall recharge thresholds in a subtropical climate determined using a regional cave drip water monitoring network. J. Hydrol., 587, 125001, 2020

Baker, A., Scheller, M., Oriani, F., Mariethoz, G., Hartmann, A., Wang, Z. and Cuthbert, M.O.: Quantifying temporal variability and spatial heterogeneity in rainfall recharge thresholds in a montane karst environment. J. Hydrol., 594, 125965, 2021.

Baker, A., Shanafield, M., Timms, W., Andersen, M. S., Priestley, S., and Melo Zurita, M.: An underground drip water monitoring network to characterize rainfall recharge of groundwater at different geologies, environments, and climates across Australia, Geosci. Instrum. Methods Data Syst., 13, 117-129, 2024

Balfour, V.N., Doerr, S.H., and Robichaud, P.R.: The temporal evolution of wildfire ash and implications for post-fire infiltration. Int. J. Wildland Fire 23, 733–745, doi:10.1071/WF13159, 2014.

Bian, F., Coleborn K., Flemons, I., Baker, A., Treble, P.C., Hughes, C.E., Baker, A., Andersen, M.S., Tozer, M.G., Duan, W., Fogwill, C.J. and Fairchild, I.J.: Hydrological and geochemical responses of fire in a shallow cave system. Sci. Total Environ., 662, 180-191, 2019.

Boas, T. and Mallants, D.: Episodic extreme rainfall events drive groundwater recharge in arid zone environments of central Australia. J. Hydrology: Regional Studies, 40, 101005, 2022.

Bodí, M.B., Martin, D.A., Balfour, V.N., Santín, C., Doerr, S.H., Pereira, P., Cerdà, A. and Mataix-Solera, J.: Wildland fire ash: Production, composition and eco-hydro-geomorphic effects. Earth-Science Rev., 130, 103–127, doi:10.1016/j.earscirev.2013.12.007, 2014

Bureau of Meteorology: Australian Water Outlook, https://awo.bom.gov.au/ access 9th December 2024

Cerdà, A.: Changes in overland flow and infiltration after a rangeland fire in a Mediterranean scrubland. Hydrol. Proc., 12, 1031–1042, doi: 10.1002/(SICI)1099-1085(19980615)12:7<1031::AID-HYP636>3.0.CO;2-V, 1998

Chen, Z., Goldscheider, N., Auler, A., Bakalowicz, M., Broda, S., Drew, D., Hartmann, J., Jiang, G., Moosdorf, N., Richts, A., Stevanovic, Z., Veni, G., Dumont, A., Aureli, A., Clos, P., and Krombholz, M.: World Karst Aquifer Map (WHYMAP WOKAM). BGR, IAH, KIT, UNESCO, doi: 10.25928/b2.21_sfkq-r406, 2017

333 Frost, A. J., and Shokri, A.: The Australian Landscape Water Balance model (AWRA-L v7). Technical Description of the
334 Australian Water Resources Assessment Landscape model version 7. Bureau of Meteorology Technical Report, 2021.

335 Gabet, E.J. and Sternberg, P.: The effects of vegetative ash on infiltration capacity, sediment transport, and the generation of
336 progressively bulked debris flows. Geomorphology, 101, 666–673, doi: 10.1016/j.geomorph.2008.03.005, 2008.

337 Guzmán-Rojo, M., Fernandez, J., d'Abzac, P. and Huysmans, M.: Impacts of Wildfires on Groundwater Recharge: A
338 Comprehensive Analysis of Processes, Methodological Challenges, and Research Opportunities. Water, 16, 2562,
339 https://doi.org/10.3390/w16182562, 2024

340 Healy, R.W. and Cook, P.G.: Using groundwater levels to estimate recharge. Hydrogeol. J., 10, 91–109, doi: 10.1007/s10040-
341 001-0178-0, 2002.

342 Kotchoni, D.O.V., Vouillamoz, JM., Lawson, F.M.A., Adjomayi, P., Boukari, M. and Taylor, R.G.: Relationships between
343 rainfall and groundwater recharge in seasonally humid Benin: a comparative analysis of long-term hydrographs in sedimentary
344 and crystalline aquifers. Hydrogeol. J., 27, 447–457, doi: 10.1007/s10040-018-1806-2, 2019.

345 Moody, J.A., Shakesby, R.A., Robichaud, P.R., Cannon, S.H. and Martin, D.A.: Current research issues related to post-wildfire
346 runoff and erosion processes. Earth Sci. Rev. 122, 10-37, 2013.

347 Noori, R., Maghrebi, M., Jessen, S., Bateni, S.M., Heggy, E., Javadi, S., Noury, M., Pistre, S., Abolfathi, S., and AghaKouchak,
348 A.: Decline in Iran's groundwater recharge. Nat. Commun., 14, 6674, doi: 10.1038/s41467-023-42411-2, 2023

349 Onda, Y., Dietrich, W.E. and Booker, F.: Evolution of overland flow after a severe forest fire, Point Reyes, California. Catena,
350 72, 13–20, doi: 10.1016/j.catena.2007.02.003, 2008.

351 Osborne, R.A.: The History of Karstification at Wombeyan Caves, New South Wales, Australia, as revealed by Palaeokarst
352 Deposits, Cave Science, 20, 1-8, 1993.

353 Pepler, A., Coutts-Smith, A. and Timbral, B.: The role of East Coast Lows on rainfall patterns and inter-annual variability
354 across the East Coast of Australia. Int. J. Climatol. 34 1011-2021, doi: 10.1002/joc.3741, 2014

355 Scott, D.F. and Van Wyk, D.B.: The effects of wildfire on soil wettability and hydrological behaviour of an afforested
356 catchment. J. Hydrol. 121, 239-256, 1990

357 Woods, S.W. and Balfour, V.N.: The effect of ash on runoff and erosion after a severe forest wildfire, Montana, USA. Int. J.
358 Wildland Fire 17, 535–548, doi: 10.1071/WF07040, 2008.

359 Wylie, J. and Wylie, G.: The caves of Wombeyan: An annotated listing. In: Caves and Karst of Wombeyan. Sydney
360 Speleological Society Occasional Paper, 13, 167-196, 2004.

361

362 **Appendix**

363

364
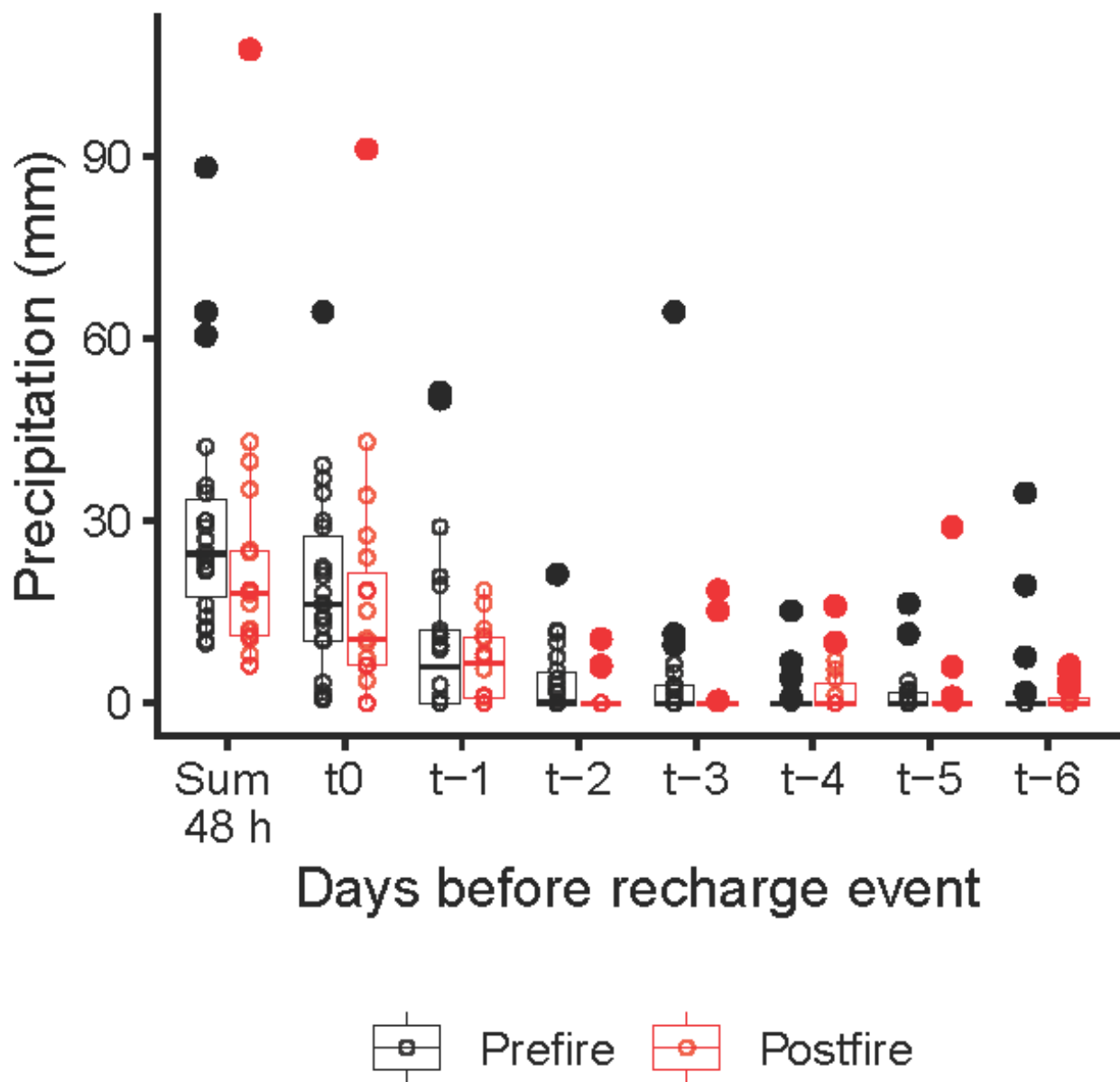
365 **Figure A1.** The amount of precipitation summed over the 48 hours prior to recharge compared to the amount of rainfall in each of the seven
366 days prior to recharge. Precipitation data is shown for recharge events pre-fire (black) and post-fire (red).
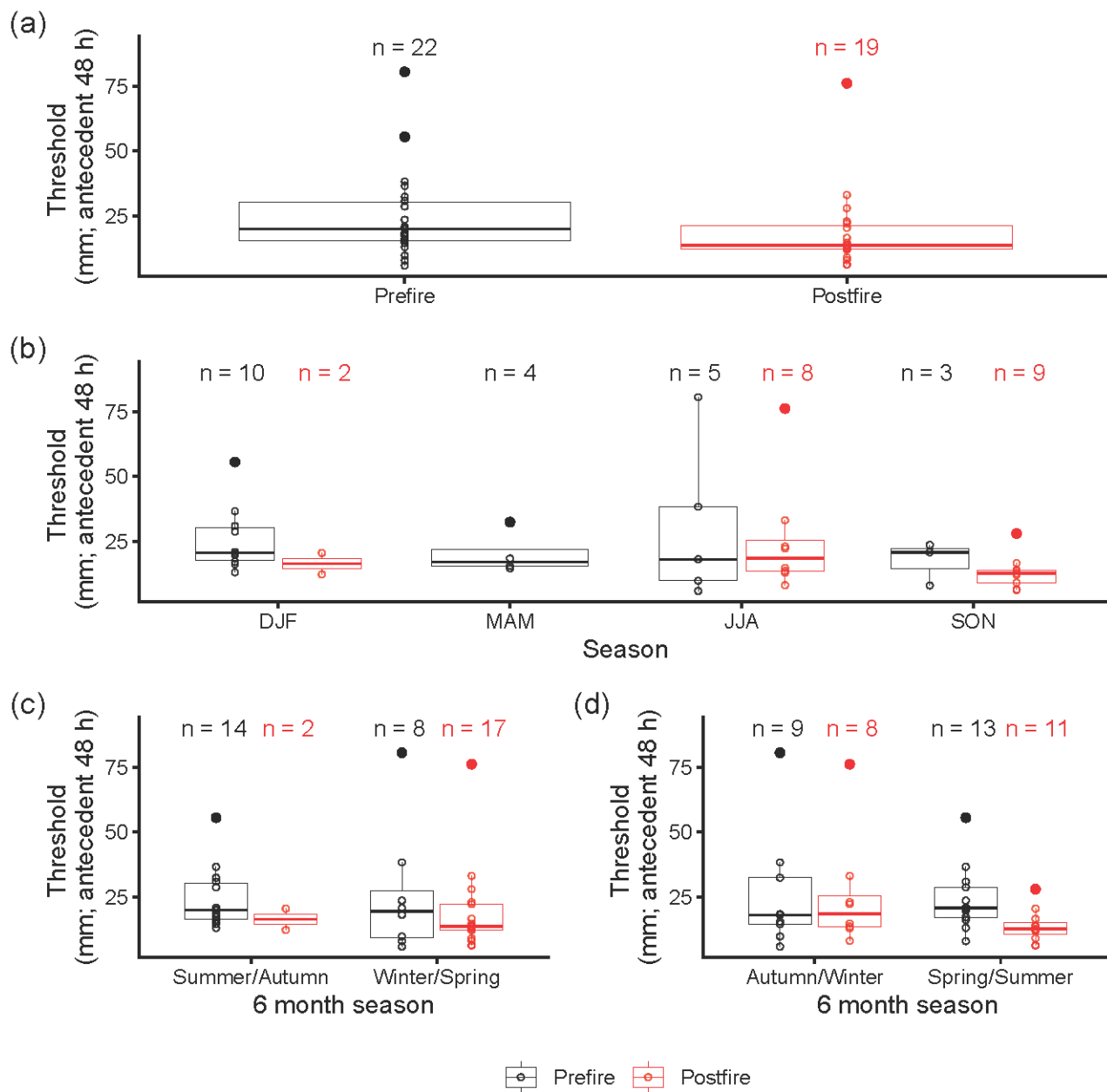367

Figure A2. Comparison of recharge thresholds pre-and post-fire using AWRA-L data. Note that sample sizes are different depending on seasonal grouping, most comparable for panel d, where Autumn/Winter have 9 samples for pre-fire, 8 samples for post-fire, and spring/summer have 13 samples for pre-fire, 11 samples for post-fire.

375

376
377 **Figure A3.** Four months post-fire Note the lack of surface ash. View is across slope, cave entrance is in foreground. Photo credit: Andy
378 Baker
379

393 **Figure A4** One year post-fire. Note lack of shrubby vegetation and patches of exposed limestone. View is downslope, Wildman's Cave is
394 beneath the foreground surface. Photo credit: Andy Baker
395